On $SU(3)_F$ positive-parity octet and decuplet baryons

Chen Chen[1,*]

[1]Institut für Theoretische Physik, Justus-Liebig-Universität Gießen, 35392 Gießen, Germany

Abstract. A continuum approach to the three valence-quark bound-state problem in quantum field theory, employing parametrisations of the necessary kernel elements, is used to compute the spectrum and Poincaré-covariant wave functions for all flavour-$SU(3)$ octet and decuplet baryons and their first positive-parity excitations. Such analyses predict the existence of nonpointlike, dynamical quark-quark (diquark) correlations within all baryons; and a uniformly sound description of the systems studied is obtained by retaining flavour-antitriplet–scalar and flavour-sextet–pseudovector diquarks. The analysis predicts the existence of positive-parity excitations of the Ξ, Ξ^*, Ω baryons, with masses, respectively (in GeV): 1.84(08), 1.89(04), 2.05(02). These states have not yet been empirically identified. This body of analysis suggests that the expression of emergent mass generation is the same in all u, d, s baryons and, notably, that dynamical quark-quark correlations play an essential role in the structure of each one. It also provides the basis for developing an array of predictions that can be tested in new generation experiments.

1 Introduction

The analysis of a baryon as a three–valence-body bound-state problem in continuum quantum field theory became possible following the formulation of a Poincaré-covariant Faddeev equation [1–5], which is depicted in Fig. 1. This approach assumes that dynamical, nonpointlike diquark correlations play an important role in baryon structure. Whilst the diquarks do not survive as asymptotic states, *viz*. they do not appear in the strong interaction spectrum [6, 7], the attraction between the quarks in the $\bar{3}$ channel draws a picture in which two quarks are always correlated as a colour-$\bar{3}$ diquark pseudoparticle, and binding is effected by the iterated exchange of roles between the bystander and diquark-participant quarks. This approach to the spectrum and interactions of baryons has been applied widely with phenomenological success, *e.g*. Refs. [8–24].

A spectrum of flavour-$SU(3)$ octet and decuplet baryons, their parity partners, and the radial excitations of these systems, was computed in Ref. [10, 17, 30] using a symmetry-preserving treatment of a vector × vector contact-interaction (SPCI) [25–29] as the foundation for the relevant few-body equations. With such an approach: the diquark bound-state amplitudes are momentum-independent but the diquarks are dynamical degrees-of-freedom with nonzero electromagnetic radii [30]; and one obtains a spectrum that is qualitatively equivalent to the quark-model and lQCD results.

In Ref. [19] we employed a QCD-kindred framework which used elsewhere [18] to perform a realistic study of the four lightest ($I = 1/2, J^P = 1/2^\pm$) baryon isospin-doublets; extended it to flavour-$SU(3)$ and delivered therewith a spectrum of octet and decuplet baryons and their first positive-parity excitations along with structural insights drawn from analyses of their Poincaré-covariant wave functions.

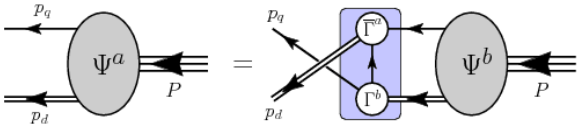

Figure 1. Poincaré covariant Faddeev equation: a linear integral equation for the matrix-valued function Ψ, being the Faddeev amplitude for a baryon of total momentum $P = p_q + p_d$, which expresses the relative momentum correlation between the dressed-quarks and -nonpointlike-diquarks within the baryon. The shaded rectangle demarcates the kernel of the Faddeev equation: *single line*, dressed-quark propagator (Sec. 2.2); Γ, diquark correlation amplitude (Sec. 2.3); and *double line*, diquark propagator (Sec. 2.4).

We emphasise that the continuum analyses indicated above form part of the body of Dyson-Schwinger equation (DSE) studies of hadron structure [29, 31–49]. In this approach, the challenge is a need to employ a truncation so as to define a tractable problem. Much has been learnt; and one may now separate DSE studies into three classes. *Class-A*. model-independent statements about QCD; *Class-B*. illustrations of such statements using well-constrained model elements and possessing a traceable connection to QCD; *Class-C*. QCD-inspired analyses whose elements have not been computed using a truncation that preserves a systematically-improvable connection with QCD. The analysis described herein lies within Class-C.

We describe our approach to the baryon bound-state problem in Sec. 2; and detail and explain the character of

*e-mail: Chen.Chen@theo.physik.uni-giessen.de

the solutions for the octet and decuplet baryons and their first positive-parity excitations in Sec. 3. Section 4 provides a summary and indicates some new directions.

2 Baryon Bound State Problem

2.1 Faddeev equation

In its general form, the Faddeev equation sums all possible exchanges and interactions that can take place between the three dressed-quarks that express a baryon's valence-quark content. Used with a realistic quark-quark interaction [50–56], it predicts the appearance of soft (nonpoint-like) fully-interacting diquark correlations within baryons, whose characteristics are greatly influenced by dynamical chiral symmetry breaking (DCSB) [13]. Consequently, the problem of determining a baryon's mass, internal structure, etc., is transformed into that of solving the linear, homogeneous matrix equation depicted in Fig. 1.

2.2 Dressed quarks

Regarding flavour-$SU(3)$ octet and decuplet baryons and their radial excitations, the Faddeev kernel in Fig. 1 involves three basic elements, *viz.* the dressed light-quark propagators, $S_f(p)$, $f = u, d, s$, and the correlation amplitudes and propagators for all participating diquarks. Much is known about $S_f(p)$, and in constructing the kernel we use the algebraic forms described in Ref. [19], which have proven efficacious in the explanation and unification of a wide range of hadron observables [11–14, 57, 58]. (*N.B.* We assume isospin symmetry throughout, *i.e.* u- and d-quarks are mass-degenerate and described by the same propagator. Consequently, all diquarks in an isospin multiplet are degenerate.)

2.3 Correlation amplitudes

In Fig. 1, all participating diquarks are colour-antitriplets because they must combine with the bystander quark to form a colour singlet.

Diquark isospin-spin structure is more complex. Accounting for Fermi-Dirac statistics, five types of correlation are possible in a $J = 1/2$ bound-state: flavour-$\bar{3}$–scalar, flavour-6–pseudovector, flavour-$\bar{3}$–pseudoscalar, flavour-$\bar{3}$–vector, and flavour-6–vector. However, only the first two are important in positive-parity systems [15, 17, 18]; and the associated leading correlation amplitudes are, respectively:

$$\Gamma^j_{0^+}(k;K) = g^j_{0^+}\,\vec{H}\,T^j_{\bar{3}_f}\,\gamma_5 C\,\mathcal{F}(k^2/[\omega^j_{0^+}]^2)\,, \tag{1a}$$

$$\Gamma^g_{1^+\mu}(k;K) = i g^g_{1^+}\,\vec{H}\,T^g_{6_f}\,\gamma_\mu C\,\mathcal{F}(k^2/[\omega^g_{1^+}]^2)\,, \tag{1b}$$

where: K is the total momentum of the correlation, k is a two-body relative momentum, $\mathcal{F}(x) = (1 - e^{-x})/x$, $\omega^{j,g}_{J^P}$ are size parameters, and $g^{j,g}_{J^P}$ are couplings into the channel, fixed by normalisation; $\vec{H} = \{i\lambda^7_c, -i\lambda^5_c, i\lambda^2_c\}$, with $\{\lambda^k_c, k = 1,\ldots,8\}$ denoting Gell-Mann matrices in colour-space, expresses the diquarks' colour antitriplet character; $C = \gamma_2\gamma_4$ is the charge-conjugation matrix;

$$\{T^j_{\bar{3}_f}, j = 1,2,3\} = \{i\lambda^2, i\lambda^5, i\lambda^7\}\,, \tag{2a}$$

$$\{T^g_{6_f}, g = 1,\ldots,6\} = \{s_0\lambda^0 + s_3\lambda^3 + s_8\lambda^8, \lambda^1, \lambda^4, s_0\lambda^0 - s_3\lambda^3 + s_8\lambda^8, \lambda^6, s_0\lambda^0 - 2s_8\lambda^8\}\,, \tag{2b}$$

with $s_0 = \sqrt{2}/3$, $s_3 = 1/\sqrt{2}$, $s_8 = 1/\sqrt{6}$, $\{\lambda^k, k = 1,\ldots,8\}$ denoting flavour-$SU(3)$ Gell-Mann matrices, $\lambda^0 = \mathrm{diag}[1,1,1]$, and all flavour matrices left-active on column$[u,d,s]$.

Turning to decuplet baryons, since it is not possible to combine a $\bar{3}_f$ diquark with a 3_f-quark to obtain a member of the symmetric 10_f representation of $SU(3)_f$, decuplet baryons only contain 6_f–axial-vector diquarks, which are associated with the amplitudes in Eq. (1b).

2.4 Diquark propagators, masses, couplings

A propagator is associated with each quark-quark correlation in Fig. 1; and we use [11, 18]:

$$\Delta^{0^+\,j}(K) = \frac{1}{[m^j_{0^+}]^2}\,\mathcal{F}(K^2/[\omega^j_{0^+}]^2)\,, \tag{3a}$$

$$\Delta^{1^+\,g}_{\mu\nu}(K) = \left[\delta_{\mu\nu} + \frac{K_\mu K_\nu}{[m^g_{1^+}]^2}\right]\frac{1}{[m^g_{1^+}]^2}\,\mathcal{F}(K^2/[\omega^g_{1^+}]^2)\,. \tag{3b}$$

These algebraic forms ensure that the diquarks are confined within the baryons, as appropriate for coloured correlations: whilst the propagators are free-particle-like at spacelike momenta, they are pole-free on the timelike axis. This is sufficient to ensure confinement via the violation of reflection positivity (see, e.g. Ref. [43], Sec. 3).

The diquark masses and sizes are related via

$$m^{j,g}_{J^P} = \sqrt{2}\,\omega^{j,g}_{J^P}. \tag{4}$$

This identification accentuates the free-particle-like propagation characteristics of the diquarks within the baryon [11]. The mass-scales are constrained by numerous studies; and we use (in GeV):

$$m^{(1)}_{0^+} = 0.80\,,\; m^{(2,3)}_{0^+} = 0.95\,, \tag{5a}$$

$$m^{(4,5,7)}_{1^+} = 0.90\,,\; m^{(6,8)}_{1^+} = 1.05\,,\; m^{(9)}_{1^+} = 1.20\,, \tag{5b}$$

where the values of $m^{(j=1)}_{0^+}$ and $m^{(g=4,5,7)}_{1^+}$ are drawn from Refs. [11, 12], because they provide for a good description of numerous dynamical properties of the nucleon, Δ-baryon and Roper resonance; and the masses $m^{(j=2,3)}_{0^+}$, $m^{(g=6,8)}_{1^+}$ and $m^{(g=9)}_{1^+}$ are derived therefrom via an equal-spacing rule, *viz.* replacing one light-quark by a s-quark brings an extra $0.15\,\mathrm{GeV} \approx M^E_s - M^E_u$ [19]. And for completeness, we will subsequently display results with all diquark masses varied by ±5%.

Using canonical normalization condition [19] and the masses in Eqs. (5):

$$g^{(1)}_{0^+} = 14.75\,,\; g^{(2,3)}_{0^+} = 9.45\,, \tag{6a}$$

$$g^{(4,5,7)}_{1^+} = 12.73\,,\; g^{(6,8)}_{1^+} = 7.62\,,\; g^{(9)}_{1^+} = 3.72\,. \tag{6b}$$

Given that it is the coupling-squared which appears in the Faddeev kernels, scalar diquarks will dominate the Faddeev amplitudes of $J = 1/2$ baryons; but pseudovector diquarks must also play a material role because $g^2_{1^+}/g^2_{0^+} \approx 0.7$, which agrees with the previous studies on the nucleon, see, *e.g.* Ref. [67, 68].

2.5 Faddeev amplitudes and wave functions

In solving the Faddeev equation, Fig. 1, one obtains both the mass-squared and bound-state amplitude of all baryons with a given value of J^P. In fact, it is the form of the Faddeev amplitude which fixes the channel. A baryon is described by

$$\Psi^B = \psi^B_1 + \psi^B_2 + \psi^B_3 , \tag{7}$$

where the subscript identifies the bystander quark, *i.e.* the quark that is not participating in a diquark correlation, $\psi^B_{1,2}$ are obtained from $\psi^B_3 =: \psi^B$ by a cyclic permutation of all quark labels.

For an octet baryon ($B_{\underline{8}} = N, \Lambda, \Sigma, \Xi$; $J^P = 1/2^+$),

$$\begin{aligned}
&\psi^{\underline{8}}(p_i, \alpha_i, \sigma_i) \\
&= \sum_{j \in B_{\underline{8}}} [\Gamma^j_{0^+}(k;K)]^{\alpha_1\alpha_2}_{\sigma_1\sigma_2} \, \Delta^{0^+ j}(K) \, [\varphi^{\underline{8}j}_{0^+}(\ell;P) u(P)]^{\alpha_3}_{\sigma_3} \\
&+ \sum_{g \in B_{\underline{8}}} [\Gamma^g_{1^+\mu}]^{\alpha_1\alpha_2}_{\sigma_1\sigma_2} \, \Delta^{1^+ g}_{\mu\nu} \, [\varphi^{\underline{8}g}_{1^+\nu}(\ell;P) u(P)]^{\alpha_3}_{\sigma_3} ,
\end{aligned} \tag{8}$$

where $(p_i, \sigma_i, \alpha_i)$ are the momentum, spin and isospin labels of the quarks constituting the bound state; $P = p_1 + p_2 + p_3 = p_d + p_q$ is the total momentum of the baryon; $k = (p_1 - p_2)/2$, $K = p_1 + p_2 = p_d$, $\ell = (-K + 2p_3)/3$; j and g are the labels in Eqs. (2) and the sums run over those flavour-combinations permitted in $B_{\underline{8}}$; and $u(P)$ is a Euclidean spinor. The remaining elements in Eq. (8) are the following matrix-valued functions:

$$\varphi^{\underline{8}j}_{0^+}(\ell;P) = \sum_{k=1}^{2} \mathfrak{s}^j_{\underline{8}k}(\ell^2, \ell\cdot P) \, \mathcal{S}^k(\ell;P) , \tag{9a}$$

$$\varphi^{\underline{8}g}_{1^+\nu}(\ell;P) = \sum_{k=1}^{6} \mathfrak{a}^{g+3}_{\underline{8}k}(\ell^2, \ell\cdot P) \, \gamma_5 \mathcal{A}^k_\nu(\ell;P) , \tag{9b}$$

where

$$\begin{aligned}
&\mathcal{S}^1 = \mathbf{I}_{\rm D} , \; \mathcal{S}^2 = i\gamma\cdot\hat{\ell} - \hat{\ell}\cdot\hat{P}\mathbf{I}_{\rm D} , \\
&\mathcal{A}^1_\nu = \gamma\cdot\ell^\perp \hat{P}_\nu , \; \mathcal{A}^2_\nu = -i\hat{P}_\nu \mathbf{I}_{\rm D} , \; \mathcal{A}^3_\nu = \gamma\cdot\hat{\ell}^\perp \hat{\ell}^\perp_\nu , \\
&\mathcal{A}^4_\nu = i\hat{\ell}^\perp_\nu \mathbf{I}_{\rm D} , \; \mathcal{A}^5_\nu = \gamma^\perp_\nu - \mathcal{A}^3_\nu , \; \mathcal{A}^6_\nu = i\gamma^\perp_\nu \gamma\cdot\hat{\ell}^\perp - \mathcal{A}^4_\nu ,
\end{aligned} \tag{10}$$

with $\hat{\ell}^2 = 1$, $\hat{P}^2 = -1$, $\ell^\perp = \hat{\ell}_\nu + \hat{\ell}\cdot\hat{P}\hat{P}_\nu$, $\gamma^\perp = \gamma_\nu + \gamma\cdot\hat{P}\hat{P}_\nu$.

Owing to the symmetry-prescribed absence of flavour-$\bar{3}$ components, the structure of decuplet baryons is simpler ($B_{\underline{10}} = \Delta, \Sigma^*, \Xi^*, \Omega$; $J^P = 3/2^+$):

$$\begin{aligned}
&\psi^{\underline{10}}_\mu(p_i, \alpha_i, \sigma_i) \\
&= \sum_{g \in B_{\underline{10}}} [\Gamma^g_{1^+\mu}]^{\alpha_1\alpha_2}_{\sigma_1\sigma_2} \, \Delta^{1^+ g}_{\mu\nu} \, [\varphi^{\underline{10}g}_{\nu\rho}(\ell;P) u_\rho(P)]^{\alpha_3}_{\sigma_3} ,
\end{aligned} \tag{11}$$

where $u_\rho(P)$ is a Rarita-Schwinger spinor; and, with $\mathcal{S}^k$ and $\mathcal{A}^k_\nu$ in Eq. (10),

$$\varphi^{\underline{10}g}_{\nu\rho}(\ell;P) = \sum_{k=1}^{8} \mathfrak{a}^{g+3}_{\underline{10}k}(\ell^2, \ell\cdot P) \, \mathcal{D}^k_{\nu\rho}(\ell;P) , \tag{12a}$$

$$\mathcal{D}^k_{\nu\rho} = \mathcal{S}^k \, \delta_{\nu\rho} , \qquad k = 1, 2 , \tag{12b}$$

$$\mathcal{D}^k_{\nu\rho} = i\gamma_5 \, \mathcal{A}^{k-2}_\nu \, \ell^\perp_\rho , \quad k = 3, \ldots, 8 . \tag{12c}$$

The (unamputated) Faddeev wave function can be computed from the amplitude specified by Eqs. (8) – (12) simply by attaching the appropriate dressed-quark and diquark propagators. It may also be decomposed in the form of Eqs. (9), (12). Naturally, the scalar functions are different, and we label them $\tilde{\mathfrak{s}}^j_{\underline{8}k}$, $\tilde{\mathfrak{a}}^g_{\underline{8}k}$, $\tilde{\mathfrak{a}}^g_{\underline{10}k}$.

Both the Faddeev amplitude and wave function are Poincaré covariant, *i.e.* they are qualitatively identical in all reference frames. Naturally, each of the scalar functions that appears is frame-independent, but the frame chosen determines just how the elements should be combined. Consequently, the manner by which the dressed-quarks' spin, S, and orbital angular momentum, L, add to form a particular J^P combination is frame-dependent: L, S are not independently Poincaré invariant.[1] The set of baryon rest-frame quark-diquark angular momentum identifications can be found in Refs. [19, 62, 63].

3 Solutions and their Properties

3.1 Masses of the dressed-quark cores

We can now report results obtained by solving the Faddeev equations for octet and decuplet baryons and their first positive-parity excitations. Our computed masses are listed in Table 1: the uncertainties indicate the response of a given mass to a coherent 5% increase/decrease in the mass-scales associated with the diquarks and dressed-quarks.

It is worth noting the emergence of a Σ-Λ mass-splitting despite the fact that we have assumed isospin symmetry, *i.e.* mass-degenerate u- and d-quarks, described by the same propagator, so that all diquarks in an isospin multiplet are degenerate. Whilst the Λ^0 and Σ^0 baryons are associated with the same combination of valence-quarks, their spin-flavour wave functions are different: the $\Lambda^0_{I=0}$ contains more of the lighter $J = 0$ diquark correlations than the $\Sigma^0_{I=1}$. It follows that the Λ^0 must be lighter than the Σ^0. Therefore, our result agrees with the prediction of the Gell-Mann–Okubo mass formula [69–71].

The computed masses and corresponding empirical results are depicted in Fig. 2. It is apparent that the computed masses are uniformly larger than the corresponding empirical values. This is because our results should be viewed as those of a given baryon's dressed-quark core, whereas the empirical values include all contributions, including

[1] The nature of the combination is also scale dependent because the definition of a dressed-quark and the character of the correlation amplitudes changes with resolving scale, ζ, in a well-defined manner [60, 61]. Our analysis is understood to be valid at $\zeta \simeq 1\,$GeV.

Table 1. Computed dressed-quark-core masses of ground-state octet and decuplet baryons, and their radial excitations. Row 1: Baryon ground-states. Row 3: First positive-parity excitations of the ground-states. Masses in rows labelled "expt." are taken from Ref. [65]. A hyphen in any position indicates that no empirically known resonance can confidently be associated with the theoretically predicted state. (All dimensioned quantities are listed in GeV.)

	Row		N	Λ	Σ	Ξ	Δ	Σ^*	Ξ^*	Ω
n=0	1	DSE	1.19(13)	1.37(14)	1.41(14)	1.58(15)	1.35(12)	1.52(14)	1.71(15)	1.93(17)
	2	expt.	0.94	1.12	1.19	1.31	1.23	1.38	1.53	1.67
n=1	3	DSE	1.73(10)	1.85(09)	1.88(11)	1.99(11)	1.79(12)	1.93(11)	2.08(12)	2.23(13)
	4	expt.	1.44(03)	$1.60^{+0.10}_{-0.04}$	1.66(03)	-	1.57(07)	1.73(03)	-	-

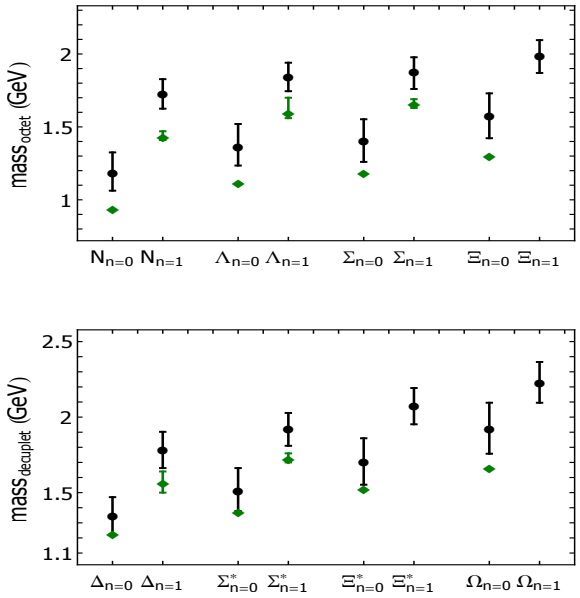

Figure 2. Upper panel: Pictorial representation of octet masses in Table 1. *Circles* (black) – computed masses. The vertical riser indicates the response of our predictions to a coherent ±5% change in the mass-scales associated with the diquarks and dressed-quarks. *Diamonds* (green) – empirical Breit-Wigner masses [65]. The horizontal axis lists a particle name with a subscript that indicates whether it is ground-state ($n = 0$) or first positive-parity excitation ($n = 1$). **Lower panel**: Analogous plot for the decuplet masses in Table 1. Where noticeable, the estimated uncertainty in the location of a resonance's Breit-Wigner mass is indicated by an error bar.

meson cloud effects, which typically generate a measurable reduction [64]. This was explained and illustrated in a study of the nucleon, its parity-partner and their radial excitations in Ref. [18]; and has also been demonstrated using the SPCI [10, 17]. Identifying the difference between our predictions and experiment, then one finds that such effects are fairly homogeneous across the spectrum:

$$\text{mean}[m^{8}_{\text{DSE}} - m^{8}_{\text{expt.}}] = 0.26(4)\,, \tag{13a}$$

$$\text{mean}[m^{10}_{\text{DSE}} - m^{10}_{\text{expt.}}] = 0.19(5)\,. \tag{13b}$$

Namely, they act to reduce the mass of ground-state octet and decuplet baryons and their first positive-parity excitations by 0.23(6) GeV.

3.2 Diquark content

The Faddeev amplitude of each baryon can be decomposed into a sum of N_{qq} terms, $\{\mathcal{F}_i, i = 1, \ldots, N_{qq}\}$, each one of which is directly identifiable with a particular diquark component. The value of N_{qq} depends on the baryon's spin-flavour structure:

	N	Λ	Σ	Ξ	Δ	Σ^*	Ξ^*	Ω
N_{qq}	14	10	14	14	8	16	16	8

. (14)

In connection with each term, we define

$$\mathbb{D}_i = \int \frac{d^4\ell}{(2\pi)^4}\, |\mathcal{F}_i(\ell^2, \ell \cdot P)|^2 \tag{15}$$

and subsequently compute

$$\mathbb{Q}_{\mathfrak{t}} = \mathbb{W}^{-1} \sum_{i \in \mathfrak{t}} \mathbb{D}_i\,, \;\; \mathbb{W} = \sum_{i=1}^{N_{qq}} \mathbb{D}_i\,, \tag{16}$$

where $\mathfrak{t}$ ranges over the $\mathfrak{s}(= 0^+)$ and $\mathfrak{a}(= 1^+)$ components of the baryon considered. Here, $\mathbb{W}$ defines a four-dimensional L^2-norm of the baryon's Faddeev amplitude and the ratios $\mathbb{Q}_{\mathfrak{t}=\mathfrak{s}^i,\mathfrak{a}^g}$ express the relative size of the contribution from each diquark correlation to this norm. The values of these fractions are one indication of the relative strengths of the various diquark components within a baryon. They are listed in Table III of Ref.[19] and depicted for the more complex octet states in Fig. 3–upper panel.

An alternative gauge is to consider the relative contribution to a given baryon's mass owing to each of the diquark components in its Faddeev amplitude. We evaluate this by computing the hadron's mass in the absence of all except the dominant diquark correlation (often the lightest possible contributor) and then introducing the remaining correlations in their order of importance, which is determined by trial-and-error. Typically, the mass obtained using only the dominant correlation is larger than the all-correlation result. (Otherwise, the Faddeev equation would suppress any new correlation.) We therefore define the relative mass-contribution of a given correlation as follows. Suppose two diquarks contribute: qq_1, qq_2, with qq_1

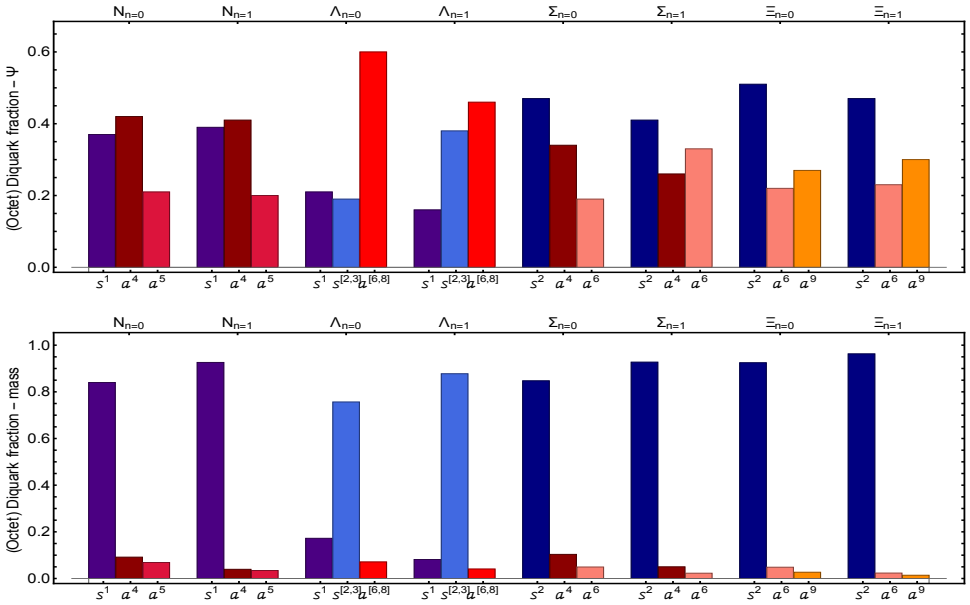

Figure 3. *Upper panel* – Relative strengths of various diquark components within the indicated baryon's Faddeev amplitude, defined via Eqs. (15), (16). *Lower panel* – Relative contribution to a baryon's mass from a given diquark correlation in that baryon's Faddeev amplitude, defined in association with Eqs. (17).

dominant. Further suppose that the qq_1-only baryon has mass m_1 and adding qq_2 gives $m_{\rm final} = m_2 < m_1$, then

$$P_1 = m_1/(m_1 + |m_2 - m_1|)\,, \tag{17a}$$
$$P_2 = |m_2 - m_1|/(m_1 + |m_2 - m_1|)\,. \tag{17b}$$

This procedure has a clear generalisation to systems with more than two diquark correlations; and the results obtained in this way are listed in Table III of Ref.[19] and depicted for the more complicated octet states in Fig. 3–lower panel.

As observed elsewhere [18], the difference between the upper and lower panels of Fig. 3 is marked. In each of the octet cases depicted in the lower panel, there is a single dominant diquark component; namely, a scalar diquark; and each new correlation adds binding, reducing the computed mass. On the other hand, measuring the relative strength of diquark correlations using the Faddeev amplitude decomposition, drawn in Fig. 3–upper panel, one arrives at a somewhat different picture; but such differences can largely be attributed to the lack of interference between diquark components in the measure defined by Eqs. (15), (16). Notwithstanding these facts, comparisons between baryons using any single measure are meaningful, *e.g.* using either scheme, the nucleon and its first positive-parity excitation possess very similar diquark content.

3.3 Rest-frame orbital angular momentum

Drawing upon Sec. 2.3, we now expose the rest-frame orbital angular momentum content of each baryon. Connected with each matrix, there is a scalar function[19, 62, 63], the collection of which we denote as $\{\mathcal{Y}_i, i = 1, \ldots, N_{qq}\}$, *e.g.* the five rest-frame ^2S-components in the proton are identified with $\mathcal{Y}_{1,\ldots,5}$ and these functions are

$$\tilde{\mathfrak{s}}^1_{N1},\ \tilde{\mathfrak{a}}^{4,5}_{N2},\ [\tilde{\mathfrak{a}}^{4,5}_{N3} + 2\tilde{\mathfrak{a}}^{4,5}_{N5}]/3. \tag{18}$$

Using this decomposition, we compiled Table 2. Plainly every one of the systems considered is primarily S-wave in nature, since they are not generated by the Faddeev equation unless S-wave components are contained in the wave function. This observation provides support in quantum field theory for the constituent-quark model classifications of these systems, so long as here angular momentum is understood at the hadronic scale to be that between the quark and diquark. Notwithstanding that, Table 2 reveals that P-wave components play a measurable role in octet ground-states and their first positive-parity excitations: they are attractive in ground-states and repulsive in the excitations. Regarding decuplet systems: the ground-state masses are almost completely insensitive to non-S-wave components; and in the first positive-parity excitations, P-wave components generate a little repulsion, some attraction is provided by D-waves, and F-waves have no measurable impact.

In order to further elucidate these remarks, we turn our attention to the Faddeev wave functions themselves and, for each baryon, compute

$$\mathbb{L}_i = \int \frac{d^4\ell}{(2\pi)^4}\, |\mathcal{Y}_i(\ell^2, \ell\cdot P)|^2, \tag{19}$$

and subsequently define the following rest-frame angular momentum strengths:

$$\begin{aligned} \mathbb{S} &= \mathbb{T}^{-1} \sum_{i\in S} \mathbb{L}_i\,, \quad \mathbb{P} = \mathbb{T}^{-1} \sum_{i\in P} \mathbb{L}_i\,, \\ \mathbb{D} &= \mathbb{T}^{-1} \sum_{i\in D} \mathbb{L}_i\,, \quad \mathbb{F} = \mathbb{T}^{-1} \sum_{i\in F} \mathbb{L}_i\,, \end{aligned} \tag{20a}$$

$$\mathbb{T} = \sum_{i=1}^{N_{qq}} \mathbb{L}_i\,. \tag{20b}$$

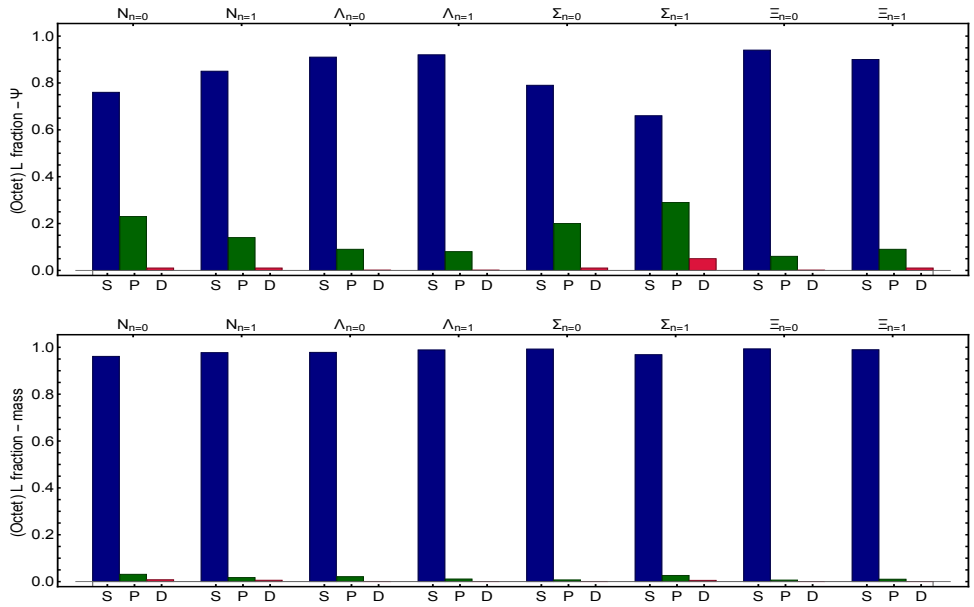

Figure 4. Octet baryons and their first positive-parity excitations. **Upper panel** – Baryon rest-frame quark-diquark orbital angular momentum fractions, as defined in Eqs. (20). **Lower panel** – Relative contribution of various quark-diquark orbital angular momentum components to the mass of a given baryon.

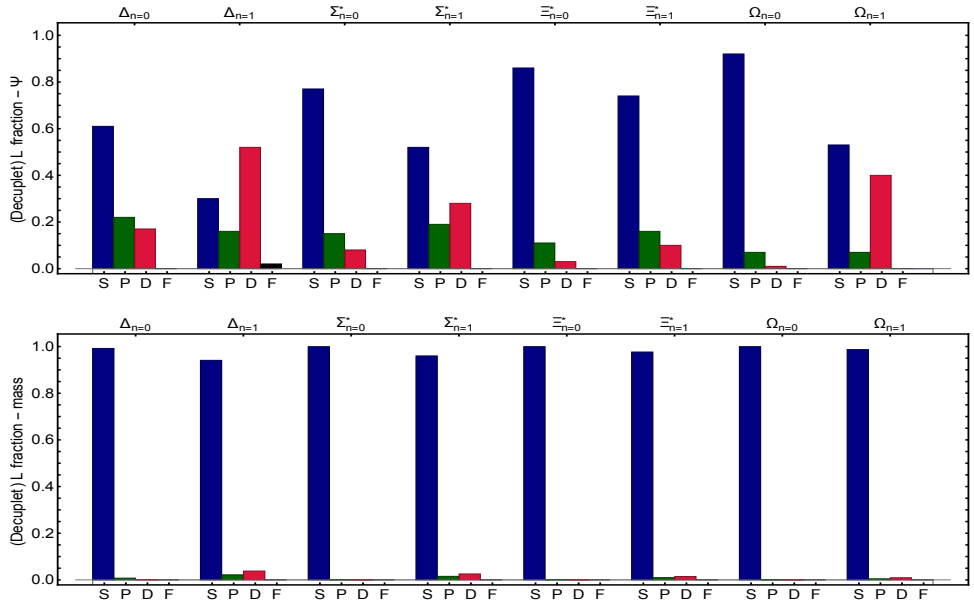

Figure 5. Decuplet baryons and their first positive-parity excitations. **Upper panel** – Baryon rest-frame quark-diquark orbital angular momentum fractions, as defined in Eqs. (20). **Lower panel** – Relative contribution of various quark-diquark orbital angular momentum components to the mass of a given baryon.

Constructed thus, $\mathbb{T}$ defines a four-dimensional L^2-norm of the baryon's rest-frame Faddeev wave function and the ratios $\mathbb{S}$, $\mathbb{P}$, $\mathbb{D}$, $\mathbb{F}$ express the relative size of the contribution from each angular momentum component to this norm. Our results are depicted in the upper panels of Figs. 4, 5.

As with our examination of the diquark content, another gauge of the relative importance of different partial waves within a baryon is to depict their contributions to a baryon's mass, which can be computed using the information in Table 2. The results are depicted in the lower panels of Figs. 4, 5. Once again, even though some contributions are repulsive and others attractive, we draw all bars as positive, following a procedure analogous to that described in connection with Eqs. (17).

Fig. 4 reveals that, concerning the rest-frame quark-diquark orbital angular momentum fractions in octet baryons, both measures deliver the same qualitative picture of each baryon's internal structure. It follows that there is little mixing between partial waves in the computation of a baryon's mass. Regarding Fig. 5, this is also

Table 2. Computed baryon quark-core masses: **upper panel**, flavour-octet; and **lower panel**, flavour-decuplet. Row 1, each panel: results obtained using the complete Faddeev wave function, *i.e*. with all angular momentum components included. Subsequent rows: masses obtained when the indicated rest-frame angular momentum component(s) is(are) excluded from the Faddeev wave function. Empty locations indicate that a solution is not obtained under the conditions indicated. (All dimensioned quantities are listed in GeV.)

L content	$N_{n=0}$	$N_{n=1}$	$\Lambda_{n=0}$	$\Lambda_{n=1}$	$\Sigma_{n=0}$	$\Sigma_{n=1}$	$\Xi_{n=0}$	$\Xi_{n=1}$
S,P,D	1.19	1.73	1.37	1.85	1.41	1.88	1.58	1.99
$-,P,D$	–	–	–	–	–	–	–	–
$S,-,D$	1.24	1.71	1.40	1.83	1.42	1.84	1.59	1.97
$S,P,-$	1.20	1.74	1.37	1.85	1.41	1.89	1.58	1.99
$S,-,-$	1.24	1.71	1.40	1.83	1.42	1.84	1.59	1.97

L content	$\Delta_{n=0}$	$\Delta_{n=1}$	$\Sigma^*_{n=0}$	$\Sigma^*_{n=1}$	$\Xi^*_{n=0}$	$\Xi^*_{n=1}$	$\Omega_{n=0}$	$\Omega_{n=1}$
S,P,D,F	1.35	1.79	1.52	1.93	1.71	2.08	1.93	2.23
$-,P,D,F$	–	–	–	–	–	–	–	–
$S,-,D,F$	1.36	1.75	1.52	1.90	1.71	2.06	1.93	2.22
$S,P,-,F$	1.35	1.82	1.52	1.95	1.71	2.09	1.93	2.24
$S,P,D,-$	1.35	1.79	1.52	1.93	1.71	2.08	1.93	2.23
$S,-,-,-$	1.35	1.80	1.52	1.93	1.71	2.08	1.93	2.23

true for the decuplet states, but there are greater quantitative dissimilarities. It is nevertheless evident in both panels that S-wave strength is shifted into D-wave contributions within decuplet positive-parity excitations, as has previously been observed [16, 59].

It is here worth contrasting these results for low-lying positive-parity baryons with those obtained elsewhere [18] for the two lightest $(I, J^P) = (1/2, 1/2^-)$ partners of the nucleon. For those systems: no solution is obtained unless P-waves are present; P-waves are the largest component of the rest-frame wave function and dominant in determining the mass, with S-waves bringing some attraction; and D-waves are negligible.

4 Summary

We computed the spectrum and Poincaré-covariant wave functions for all flavour-$SU(3)$ octet and decuplet baryons and their first positive-parity excitations (Sec. 3.1). A basic prediction of such Faddeev equation studies is the presence of strong nonpointlike, fully-interacting quark-quark (diquark) correlations within all baryons; and our analysis confirms that for a realistic description of these states, it is necessary and sufficient to retain only flavour-$\bar{3}$–scalar and flavour-6–pseudovector correlations (Sec. 3.2). Namely, negative-parity diquarks are negligible in these positive-parity baryons. Moreover, in its rest-frame, every system considered may be judged as primarily S-wave in character (Sec. 3.3).

In arriving at these conclusions, we draw a similar picture to quark model descriptions of these systems, so long as rest-frame orbital angular momentum is identified with that existing between dressed-quarks and -diquarks, which are the correct strong-interaction quasiparticle degrees-of-freedom at the hadronic scale and on a material domain extending beyond. In addition, we confirm the quark-model result that each ground-state octet and decuplet baryon possesses a radial excitation and consequently predict the existence of positive-parity excitations of the Ξ, Ξ^*, Ω baryons.

Acknowledgements

I am grateful to R. W. Gothe for convening the session in which this perspective was presented. The material contained herein is the product of collaborations with many people, to all of whom I am greatly indebted. This work was partly supported by the Helmholtz International Center for FAIR within the LOEWE program of the State of Hesse and by the DFG grant FI 970/11-1.

References

[1] R. T. Cahill, C. D. Roberts and J. Praschifka, Austral. J. Phys. **42**, 129 (1989).
[2] C. J. Burden, R. T. Cahill and J. Praschifka, Austral. J. Phys. **42**, 147 (1989).
[3] R. T. Cahill, Austral. J. Phys. **42**, 171 (1989).
[4] H. Reinhardt, Phys. Lett. B **244**, 316 (1990).
[5] G. V. Efimov, M. A. Ivanov and V. E. Lyubovitskij, Z. Phys. C **47**, 583 (1990).
[6] A. Bender, C. D. Roberts and L. von Smekal, Phys. Lett. B **380**, 7 (1996).
[7] M. S. Bhagwat, A. Höll, A. Krassnigg, C. D. Roberts and P. C. Tandy, Phys. Rev. C **70**, 035205 (2004).
[8] C. Chen *et al.*, Phys. Rev. D **99**, 034013 (2019).
[9] C. Mezrag, J. Segovia, L. Chang and C. D. Roberts, Phys. Lett. B **783**, 263 (2018).
[10] C. Chen, L. Chang, C. D. Roberts, S.-L. Wan and D. J. Wilson, Few Body Syst. **53**, 293 (2012).
[11] J. Segovia, I. C. Cloët, C. D. Roberts and S. M. Schmidt, Few Body Syst. **55**, 1185 (2014).
[12] J. Segovia *et al.*, Phys. Rev. Lett. **115**, 171801 (2015).
[13] J. Segovia, C. D. Roberts and S. M. Schmidt, Phys. Lett. B **750**, 100 (2015).
[14] J. Segovia and C. D. Roberts, Phys. Rev. C **94**, 042201(R) (2016).
[15] G. Eichmann, C. S. Fischer and H. Sanchis-Alepuz, Phys. Rev. D **94**, 094033 (2016).
[16] G. Eichmann, Few Body Syst. **58**, 81 (2017).
[17] Y. Lu *et al.*, Phys. Rev. C **96**, 015208 (2017).
[18] C. Chen *et al.*, Phys. Rev. D **97**, 034016 (2018).
[19] C. Chen, G. I. Krein, C. D. Roberts, S. M. Schmidt and J. Segovia, Phys. Rev. D **100**, no. 5, 054009 (2019).
[20] Z. F. Cui *et al.*, Phys. Rev. D **102**, no.1, 014043 (2020).
[21] J. Rodríguez-Quintero *et al.*, [arXiv:1909.13793 [nucl-th]].

[22] J. Segovia, C. Chen, Z. F. Cui, Y. Lu and C. D. Roberts, AIP Conf. Proc. **2249**, no.1, 020010 (2020).
[23] I. G. Aznauryan *et al.*, Int. J. Mod. Phys. E **22**, 1330015 (2013).
[24] M. Y. Barabanov *et al.*, [arXiv:2008.07630 [hep-ph]].
[25] C. Chen, L. Chang, C. D. Roberts, S. M. Schmidt, S. Wan and D. J. Wilson, Phys. Rev. C **87**, 045207 (2013).
[26] S. S. Xu, C. Chen, I. C. Cloet, C. D. Roberts, J. Segovia and H. S. Zong, Phys. Rev. D **92**, no. 11, 114034 (2015).
[27] J. Segovia, C. Chen, I. C. Cloët, C. D. Roberts, S. M. Schmidt and S. Wan, Few Body Syst. **55**, 1-33 (2014).
[28] J. Segovia, C. Chen, C. D. Roberts and S. Wan, Phys. Rev. C **88**, no.3, 032201 (2013).
[29] P. L. Yin, C. Chen, G. Krein, C. D. Roberts, J. Segovia and S. S. Xu, Phys. Rev. D **100**, no. 3, 034008 (2019).
[30] H. L. L. Roberts, A. Bashir, L. X. Gutiérrez-Guerrero, C. D. Roberts and D. J. Wilson, Phys. Rev. C **83**, 065206 (2011).
[31] C. D. Roberts and A. G. Williams, Prog. Part. Nucl. Phys. **33**, 477 (1994).
[32] C. D. Roberts and S. M. Schmidt, Prog. Part. Nucl. Phys. **45**, S1 (2000).
[33] P. Maris and C. D. Roberts, Int. J. Mod. Phys. E **12**, 297 (2003).
[34] C. D. Roberts, M. S. Bhagwat, A. Höll and S. V. Wright, Eur. Phys. J. ST **140**, 53 (2007).
[35] P. Boucaud *et al.*, Few Body Syst. **53**, 387 (2012).
[36] C. D. Roberts, J. Phys. Conf. Ser. **706**, 022003 (2016).
[37] A. C. Aguilar, D. Binosi and J. Papavassiliou, Front. Phys. China **11**, 111203 (2016).
[38] M. R. Pennington, J. Phys. G **43**, 054001 (2016).
[39] C. Mezrag, H. Moutarde and J. Rodríguez-Quintero, Few Body Syst. **57**, 729 (2016).
[40] G. Eichmann *et al.*, Prog. Part. Nucl. Phys. **91**, 1 (2016).
[41] C. S. Fischer, Prog. Part. Nucl. Phys. **105**, 1 (2019).
[42] C. Chen, L. Chang, C. D. Roberts, S. Wan and H. S. Zong, Phys. Rev. D **93**, no. 7, 074021 (2016).
[43] T. Horn and C. D. Roberts, J. Phys. G. **43**, 073001 (2016).
[44] F. E. Serna, C. Chen and B. El-Bennich, Phys. Rev. D **99**, no. 9, 094027 (2019).
[45] A. C. Aguilar *et al.*, Eur. Phys. J. A **55** (2019) no.10, 190.
[46] J. Segovia, C. Chen, Z. F. Cui, Y. Lu and C. D. Roberts, [arXiv:1911.04923 [nucl-th]].
[47] C. Shi *et al.*, Phys. Rev. D **92** (2015), 014035.
[48] C. Chen and C. Shi, EPJ Web Conf. **113** (2016), 05013.
[49] S. X. Qin, C. Chen, C. Mezrag and C. D. Roberts, Phys. Rev. C **97**, no. 1, 015203 (2018).
[50] M. Hopfer, A. Windisch and R. Alkofer, PoS **ConfinementX**, 073 (2012).
[51] D. Binosi, L. Chang, J. Papavassiliou and C. D. Roberts, Phys. Lett. B **742**, 183 (2015).
[52] R. Williams, C. S. Fischer and W. Heupel, Phys. Rev. D **93**, 034026 (2016).
[53] D. Binosi, L. Chang, J. Papavassiliou, S.-X. Qin and C. D. Roberts, Phys. Rev. D **95**, 031501(R) (2017).
[54] D. Binosi, C. Mezrag, J. Papavassiliou, C. D. Roberts and J. Rodríguez-Quintero, Phys. Rev. D **96**, 054026 (2017).
[55] A. K. Cyrol, M. Mitter, J. M. Pawlowski and N. Strodthoff, Phys. Rev. D **97**, 054006 (2018).
[56] J. Rodríguez-Quintero *et al.*, Few Body Syst. **59**, 121 (2018).
[57] M. A. Ivanov, Yu. L. Kalinovsky and C. D. Roberts, Phys. Rev. D **60**, 034018 (1999).
[58] M. A. Ivanov, J. G. Körner, S. G. Kovalenko and C. D. Roberts, Phys. Rev. D **76**, 034018 (2007).
[59] S.-X. Qin, C. D. Roberts and S. M. Schmidt, Phys. Rev. D **97**, 114017 (2018).
[60] G. P. Lepage and S. J. Brodsky, Phys. Rev. D **22**, 2157 (1980).
[61] K. Raya *et al.*, Phys. Rev. D **93**, 074017 (2016).
[62] M. Oettel, G. Hellstern, R. Alkofer and H. Reinhardt, Phys. Rev. C **58**, 2459 (1998).
[63] I. C. Cloët, A. Krassnigg and C. D. Roberts, [arXiv:0710.5746 [nucl-th]].
[64] N. Suzuki *et al.*, Phys. Rev. Lett. **104**, 042302 (2010).
[65] M. Tanabashi *et al.*, Phys. Rev. D **98**, 030001 (2018), (*Particle Data Group*).
[66] C. D. Roberts, Few Body Syst. **58**, 5 (2017).
[67] C. Hanhart and S. Krewald, Phys. Lett. B **344**, 55-60 (1995).
[68] A. Buck and H. Reinhardt, Phys. Lett. B **356**, 168-174 (1995).
[69] M. Gell-Mann, "The Eightfold Way: A Theory of strong interaction symmetry", Tech. Rep. TID-12608; CTSL-20.
[70] S. Okubo, Prog. Theor. Phys. **27**, 949-966 (1962).
[71] S. Okubo, Prog. Theor. Phys. **28**, 24-32 (1962).